Remanent magnetization plots of fine particles with competing cubic and uniaxial anisotropies

J. Geshev,[a] M. Mikhov,[b] and J. E. Schmidt
Instituto de Física, Universidade Federal do Rio Grande do Sul, C.P. 15051, 91501-970 Porto Alegre, RS, Brazil

(Received 11 January 1999; accepted for publication 10 February 1999)

Magnetization and remanent magnetization curves for noninteracting single-domain particles whose anisotropy is made up of a cubic magnetocrystalline and an uniaxial components were investigated. For a given cubic anisotropy, the saturation remanence, coercivity, remanence coercivity, and coercivity factor values have been obtained for several different uniaxial anisotropy directions. The corresponding δM plots have been constructed for initially thermal or ac demagnetized systems, and a great variety of their shapes has been obtained when the uniaxial anisotropy does not dominate. Coercivity factor values rather higher than those for pure uniaxial or cubic anisotropy particles have been obtained as well, even for already dominating uniaxial anisotropy for some uniaxial anisotropy directions. Thus, it has been shown that one may not safely draw conclusions about interactions from deviations from the zero line in the δM plots or coercivity factor values for particles with competing anisotropies without specific analysis for any particular case. © *1999 American Institute of Physics.* [S0021-8979(99)04310-8]

I. INTRODUCTION

During recent years, remanent magnetization measurements have been extensively used for estimation of interaction effects in fine-particle systems. The technique is based on a comparison of the principal remanence curves, the isothermal remanent magnetization curve, $M_r(H)$, and the dc demagnetization remanence curve, $M_d(H)$. The $M_r(H)$ curve is obtained on an initially demagnetized sample by applying a positive magnetic field H which is then removed and the remanence M_r is measured. A larger field is then applied and the process is repeated until saturation is reached. The $M_d(H)$ curve is measured by first saturating the sample in a positive field and then measuring the remanence M_d after application of progressively larger negative fields. Unless otherwise stated, all remanence curves are normalized to the saturation remanence. For a system of noninteracting single-domain particles with uniaxial anisotropy the $M_r(H)$ and $M_d(H)$ are connected via the Wohlfarth relation[1]

$$M_d(H)=1-2M_r(H). \tag{1}$$

Henkel[2] noted that the variation of $M_d(H)$ with $M_r(H)$ measured for heterogeneous alloys gave plots showing positive or negative curvature.

The $M_r(H)$ curve depends on the method by which the demagnetized state is produced,[3–5] as from dc, ac, or thermal demagnetization one can obtain very different initial magnetization and $M_r(H)$ curves. The noninteracting case for ac or thermal demagnetized state corresponds to a linear Henkel plot with a slope of -2. In 1989, Kelly *et al.*[6] have used the remanence curves to estimate interactions in granular thin films, due to the so-called δM plot, which is a direct measure of the deviation from the linearity;

$$\delta M=M_d(H)-1+2M_r(H). \tag{2}$$

Negative δM are usually taken to indicate ''demagnetizing'' interactions in the sense that the interactions have the effect to stabilize the demagnetized state, for example, by formation of flux closure structures. Positive values of δM are usually attributed to interactions promoting the magnetized state.

The Wohlfarth relation, derived originally for uniaxial single-domain particles, was expected to hold for multidomain ferromagnets as well, if the coercivity is greater than the field required to sweep a domain wall through a grain.[7] Henkel plots representing domain wall motion have been calculated using the classical Preisach model,[8] assuming that up-switching fields of magnetization elements are independent of down-switching fields. Starting from ac demagnetized state, the Henkel plots was shown to follow a square-root low $M_d(H)=1-2\sqrt{M_r(H)}$ for any factorizable Preisach function. Using the domain wall model of hysteresis for a variety of material correlation length values, McMichael *et al.*[9] have shown that both positive and negative δM deviations can be obtained without interactions, which depend on the demagnetization method.

Another cause for nonlineality, pointed out by Wohlfarth in his paper,[1] is nonuniaxial anisotropy. More attention should be paid to this case since the recent developments of the technology makes it possible that fine-particle materials with dominant cubic anisotropy can easily be produced (see, e.g., Ref. 10).

Henkel plots, calculated for the case of randomly orientated noninteracting spherical particles with cubic anisotropy (3 and 4 easy magnetization axes) are nonlinear in a ''posi-

[a]Electronic mail: julian@if.ufrgs.br
[b]M. Mikhov is on leave from the Faculty of Physics, ''St. Kliment Ohridski'' University of Sofia, 1126 Sofia, Bulgaria.

tive'' sense with the curves concave downwards, leading to positive δM plots.[11] The shape of the δM plots, in this case, depends on the demagnetization state as well. The δM^{dc} plot (the initial state in the acquisition of $M_r(H)$ curve is dc demagnetization) for the case of 4 easy axes has been calculated and compared with the experimental one for a face-centered-cubic (fcc) Co granular system.[12]

However, the remanence curve technique (defined for systems of uniaxial anisotropy) has been often applied, without any modifications, to systems consisting of particles with mixed multiaxial and uniaxial anisotropies. This situation arises, e.g., in iron or fcc cobalt particles having additional shape or strain anisotropy. Ultrathin films also provide conditions where uniaxial and cubic anisotropies coexist. The validity of conclusions about interactions drawn from the deviations from the zero line of δM plots for particles with competing anisotropies is, at least, doubtful.

Results for the remanence of particles having mixed uniaxial and cubic anisotropies were obtained by Tonge and Wohlfarth.[13] Recent studies on such particulate systems[14,15] revealed some interesting features, e.g., some of the particles can have negative remanent magnetization contribution.

Sometimes another parameter, derived from the hysteresis curves and the dc demagnetization remanence curve, is used for estimation the interparticle interaction effects, the so-called coercivity factor (CF),[16] defined as

$$\mathrm{CF}=(H_r/H_c-1)\times 100. \tag{3}$$

For noninteracting fine-particle systems with uniaxial anisotropy CF≈9%,[16] and for cubic anisotropy the corresponding values are CF≈4% for $K_1<0$ and CF≈6% for $K_1>0$.[11] Deviations of experimentally obtained CF values from the above theoretical ones are attributed to interparticle interactions.

In this article, we present model calculations of the magnetization and remanence curves for a disordered system of noninteracting single-domain particles with competing uniaxial and a cubic anisotropies. Various directions of the uniaxial anisotropy, and different ratios between the cubic magnetocrystalline and the uniaxial anisotropy constants have been considered.

II. MODEL

Consider a system consisting of noninteracting single-domain particles whose anisotropy is made up of a cubic magnetocrystalline and an uniaxial components. Let the direction cosines of the magnetization vector $\mathbf{M}_s$ of such a particle be α_1, α_2 and α_3 and those of the uniaxial anisotropy l, m and n, referred to the cube axes. For fixed magnitude and direction of the applied field $\mathbf{H}$, the total reduced free energy of the particle can be written as

$$\eta(\gamma,\vartheta)=\frac{E}{2|K_1|V}=\frac{1}{2}\mathrm{sign}(K_1)(\alpha_1^2\alpha_2^2+\alpha_2^2\alpha_3^2+\alpha_3^2\alpha_1^2) - \frac{K_u}{2|K_1|}(\alpha_1 l+\alpha_2 m+\alpha_3 n)^2-h\cos\phi. \tag{4}$$

Here E is the total energy, V the particle volume, K_1 the first-order magnetocrystalline anisotropy constant, h the reduced magnetic field ($=HM_s/2|K_1|$), K_u the uniaxial anisotropy constant which is here taken to be positive, and $\cos\phi$ is given by

$$\cos\phi=\cos\gamma\cos\theta+\sin\gamma\sin\theta\cos(\vartheta-\psi). \tag{5}$$

γ and ϑ are the spherical coordinates of $\mathbf{M}_s$, and θ and ψ are those of $\mathbf{H}$; ϕ is the angle between $\mathbf{M}_s$ and $\mathbf{H}$.

In zero applied field and $K_u=0$, it is possible to analytically determine which are the easy magnetization directions. When $K_1>0$, there are six energy minima along the principal cube axes, i.e., the equivalent easy directions are of the type $\langle 100\rangle$. The maxima are eight orientations of the type $\langle 111\rangle$ along the body diagonals. When $K_1<0$, the maxima and minima orientations obtained for $K_1>0$ are interchanged. Thus there are eight easy directions of the type $\langle 111\rangle$ and six maxima of the type $\langle 100\rangle$. In general, with the increase of $K_u/|K_1|$ these minima move towards the $[l,m,n]$ direction and they reach this direction only when $K_u/|K_1|\rightarrow\infty$.

In the presence of an applied field, the energy function is more difficult to minimize and the equations can only be solved numerically. The two-variable minimization procedure used in the present work is described elsewhere.[15] Here, the method was modified for the remanence curves calculations. After the application of H, to obtain the corresponding remanent magnetization value, the field has not been removed at once, but has been decreased to zero in the same steps as in the magnetization curve acquisition process. It was assumed that the particles' magnetizations can become trapped in local energy minima, no matter how shallow (i.e., the thermal activation effects are neglected). Special care was taken to avoid getting hung up when a local minimum turns into a saddle point.

Three distinct initial magnetization states were used for the calculation of the initial magnetization curves, $M_r(H)$ and the resulting δM plots. The ''thermal demagnetized'' state is usually obtained in the experiments by heating the system above its Curie temperature, followed by quenching in zero magnetic field, which ''freezes'' in random occupation probabilities for each equilibrium state for the particles' magnetizations. In the present model calculations, the occupation probabilities are taken to be of 1/2 when the number of minimum energy directions is reduced to 2, and when the cubic anisotropy still dominates over the uniaxial one these are of 1/6 for $K_1>0$ and of 1/8 for $K_1<0$.

The ac demagnetized state is experimentally achieved by continuous cyclic erasure from saturation, which leaves only the lowest energy state occupied. Here this state is realized by assuming that the initial positions of the particles' magnetizations are these with lowest energy.

The dc demagnetized state is obtained by first saturating the sample in a positive direction, applying the remanent coercive field in the negative direction and then returning the field to zero, yielding $M=0$.

Curves obtained after dc demagnetization (except the curve in Fig. 1) will not be considered in the present article.

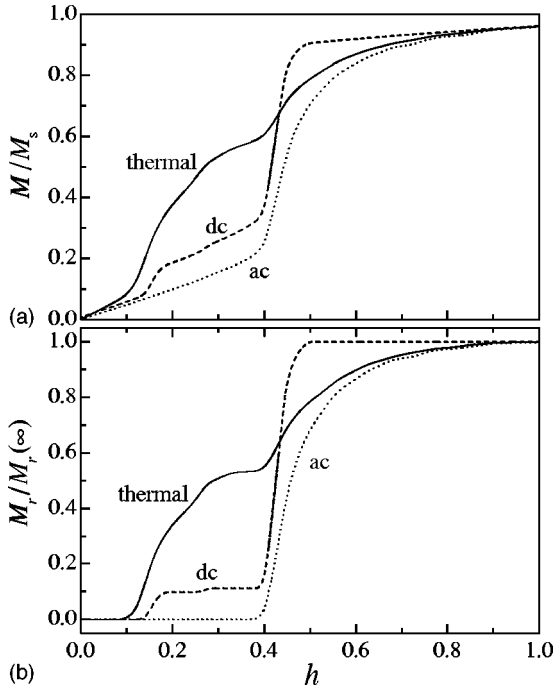

FIG. 1. (a) Representative initial magnetization curves and (b) the corresponding remanence curves calculated for ac, dc, and ''thermal demagnetization'' methods, for one particular case: $[l,m,n]$ direction given by [100], $K_1>0$, and $K_u/K_1=0.4$.

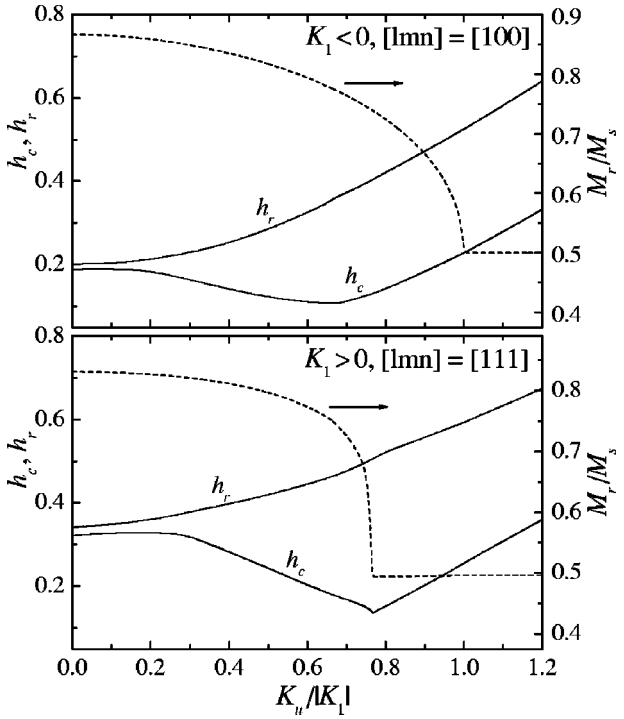

FIG. 2. Reduced coercivity, remanence coercivity, and saturation remanence vs $K_u/|K_1|$ when the $[l,m,n]$ direction is along a hardest cubic anisotropy axis.

III. RESULTS AND DISCUSSION

Figure 1 shows representative initial magnetization curves and the corresponding remanence curves calculated for one particular case: $[l,m,n]$ direction given by [100], $K_1>0$ and $K_u/K_1=0.4$, for the above mentioned three distinct demagnetization states. As it can be seen from the figure, the initial magnetization curves, as well as the remanence curves, differ significantly.

The cases when $[l,m,n]$ is along the hardest, easiest and intermediate cubic anisotropy axes have been considered, as well as the case when $[l,m,n]$ is given by [112] direction. For each case, the ratio $K_u/|K_1|$ was varied and the initial magnetization curve, hysteresis loop, and the remanence curves were calculated for any $K_u/|K_1|$ value. The coercivity, h_c, and remanence coercivity, h_r, $[M_d(h_r)=0]$ were extracted from these curves, and the δM plots were constructed using the remanent magnetization curves. Here the coercivities are reduced to $2|K_1|/M_s$ for $K_1\neq 0$, and to $2K_u/M_s$ when $K_1=0$. A more detailed analysis of these cases is given below.

A. $[l,m,n]$ direction along a hardest cubic anisotropy axis

In this case, the uniaxial anisotropy direction is given by [100] direction for $K_1<0$ and by [111] direction when $K_1>0$. The coercivity, remanence coercivity, and saturation remanence versus $K_u/|K_1|$ dependencies are shown in Fig. 2 for both positive and negative K_1.

The dependencies of M_r/M_s on $[l,m,n]$ direction have already been calculated for various values of $K_u/|K_1|$.[15] It has been shown that when the uniaxial anisotropy dominates over the cubic one, i.e. the number of minimum energy directions is reduced to 2, there are only three cases for which $M_r/M_s=0.5$. These are: $[l,m,n]$ directions given by $\langle 100\rangle$ or $\langle 110\rangle$ for $K_1>0$, and $\langle 110\rangle$ for $K_1<0$. For all other cases, $M_r/M_s<0.5$ and reaches 0.5 only when $K_u/|K_1|\to\infty$. The lower than 0.5 reduced remanence for systems with competing anisotropies comes from the negative remanent magnetization contribution of some of the particles.

The most interesting new results, presented in Fig. 2, are the minima in the h_c dependencies. This could be explained as follows.

As mentioned above, at zero field and zero K_u there are eight minima along the $\langle 111\rangle$ directions when $K_1<0$ and six minima, along the $\langle 100\rangle$ directions, when $K_1>0$. When K_u is raised, the energy along these axes decreases because the uniaxial anisotropy is along one of the hardest cubic anisotropy axes. The depth of the minima changes and so does their locations: two groups of minima are formed, one of them approaching the $[l,m,n]$ direction and the other one approaching the $[\bar{l},\bar{m},\bar{n}]$ direction. Starting from the saturation remanence state, once a reverse field is applied, the energies at each of these minima changes and they are no longer equal. At still higher field strengths some of the minima start to be eliminated as the field energy starts to become dominant. For some particle configurations (i.e., the specific orientation of the particles in relation to the field direction), the magnetization jumps to other minimum in the same group, closer to the field direction, thus increasing its (negative) contribution to the system's total magnetization. I.e., the fields necessary for these irreversible transitions over the corresponding energy barriers are decreased, compared to

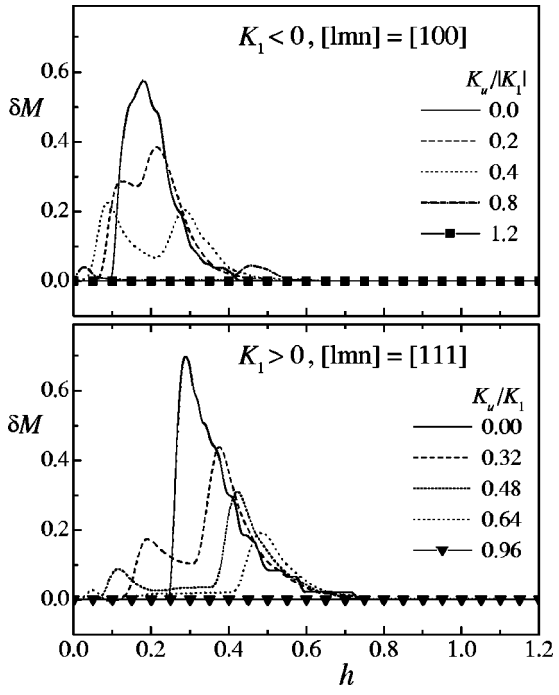

FIG. 3. Representative δM plots when the $[l,m,n]$ direction is along a hardest cubic anisotropy axis.

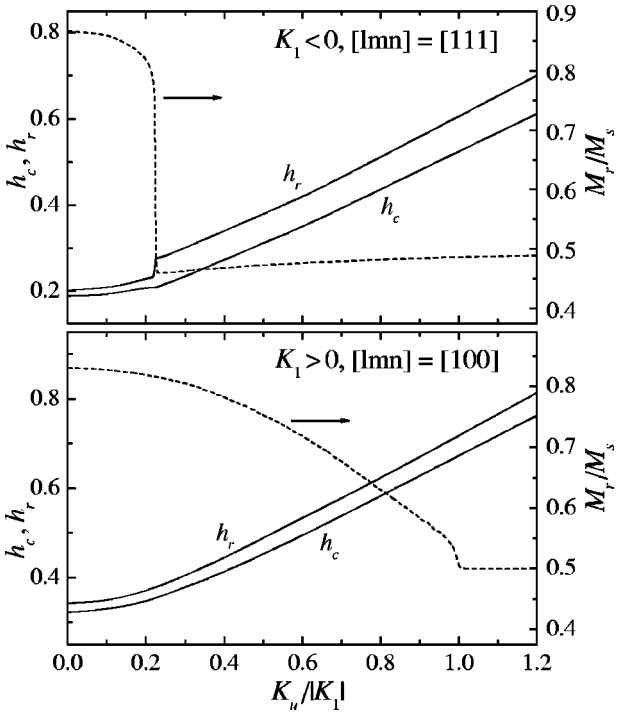

FIG. 4. Reduced coercivity, remanence coercivity, and saturation remanence vs $K_u/|K_1|$ for $[l,m,n]$ along a easiest cubic anisotropy axis.

the ones for lower K_u values, and so does the coercivity of the system. Further raise of K_u leads to that the first irreversible rotations occur at lower field, but also approximates even more the energy minima, so the decrease of the total magnetization is relatively smaller. This, together with the continuous increase of the energy barrier for the second irreversible jumps (to the vicinity of the $[\bar{l},\bar{m},\bar{n}]$ direction), leads to the subsequent increase of h_c.

Although minima in $h_r(K_u/|K_1|)$ for some particle's orientations were observed, there are no minima in the total h_r dependencies. Using the calculated remanence curves, the corresponding δM plots can be constructed following Eq. (2). Some representative δM plots are shown in Fig. 3. In this case, due to the equivalency of the energy minima there is no difference in the $M_r(H)$ obtained after ac or thermal demagnetization. (Such a difference could exist if the interparticle interactions are not negligible.) Thus, there is only one type of δM plots. Values of $K_u/|K_1|$ high enough, so that the uniaxial anisotropy to dominate over the cubic one, lead to $\delta M(H)=0$. It should also be stressed that for dominant cubic anisotropy, only positive δM values are observed, as for the case of pure cubic anisotropy.[11]

Another interesting feature is the presence of two maxima for all plots (except for the case of $K_u=0$) for dominating cubic anisotropy. This accounts for the particular field dependencies of both $M_r(H)$ and $M_d(H)$ curves. In low fields, the critical fields for the first irreversible changes during the initial magnetization process are lower than the corresponding fields during the demagnetization process, as it is for the $K_u=0$ case.[11] The $M_r(H)$ increases while $M_d(H)$ remains constant, resulting in the initial increase in the δM plots. Further raise of the reverse field causes the first irreversible rotations during the demagnetization, as described above, resulting in the $M_r(H)$ decrease and thus the δM decrease. After these first irreversible changes during demagnetization take place, the remanence curves tend to have behavior similar to those for the case of $K_u=0$; as it can be seen from the figure, after reaching the second maxima, the δM curves follow approximately the plot for the $K_u=0$ case.

B. $[l,m,n]$ direction along an easiest cubic anisotropy axis

Now, [111] is the uniaxial anisotropy direction when $K_1<0$, and [100] when $K_1>0$. The h_c, h_r and M_r/M_s vs $K_u/|K_1|$ dependencies are shown in Fig. 4. No peculiarities in the curves were observed except a small step in the h_r curve due to the very sharp transition from the state with multiaxial anisotropy to the state with 2 energy minima.

When K_u is raised, even at zero field there are two global energy minima along the $[l,m,n]$ direction, while the others are local ones. The initial magnetization and $M_r(H)$ curves, and subsequently the corresponding δM plots, obtained after ac and thermal demagnetization, are different in the present case. This is demonstrated in Fig. 5 where some representative δM plots are shown. It should be noted that when the cubic anisotropy still dominates over the uniaxial one, the plots obtained after thermal demagnetization show positive deviations only. δM^{ac} plots, however, for negative K_1, show both positive and negative deviations, and when K_1 is positive there are only negative plots.

There are several reasons for these differences. For positive K_1 and $K_u\neq 0$, the depth of the local minima decreases, but their locations do not change. This is not true for $K_1<0$ when the energy surface is distorted by the uniaxial anisotropy and the local minima are not equivalent; like in the

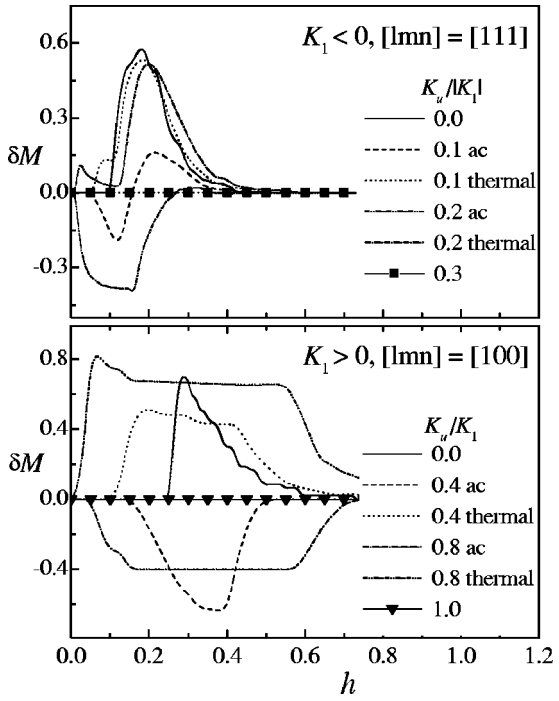

FIG. 5. Representative δM plots when the $[l,m,n]$ direction is along an easiest cubic anisotropy axis.

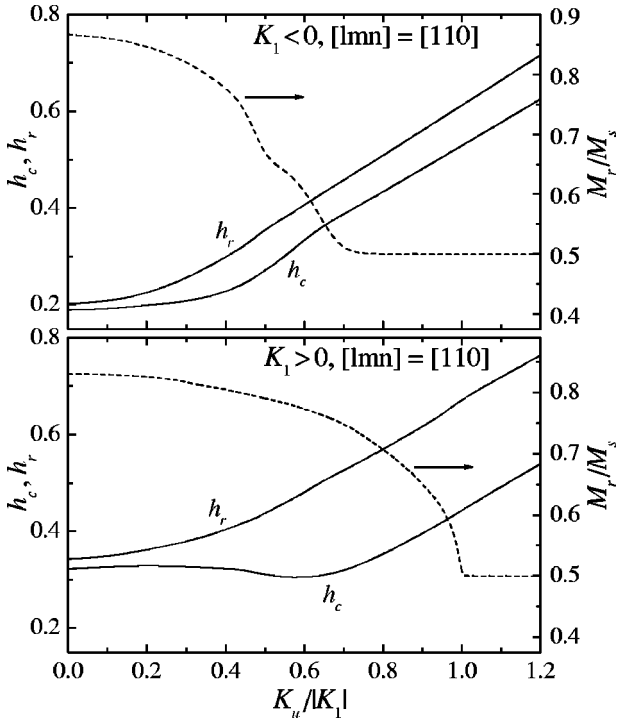

FIG. 6. Reduced coercivity, remanence coercivity, and saturation remanence vs $K_u/|K_1|$ for $[l,m,n]$ along an intermediate cubic anisotropy axis.

case with $[l,m,n]$ direction along a magnetocrystalline hardest axis, two groups of minima are formed, each of them approaching the $[l,m,n]$ direction and the reverse one, respectively. Moreover, there are less minima for $K_1>0$ than for $K_1<0$, so there are different numbers of possible magnetization jumps during the magnetization processes for the two cases.

Using argumentation similar to that in the above subsection, the peculiarities in the different types of curves in this and in the next two subsections could be explained.

C. $[l,m,n]$ direction along an intermediate cubic anisotropy axis

This is the [110] direction for both cases of positive and negative cubic anisotropy constant. The reduced coercivity, remanence coercivity, and saturation remanence versus $K_u/|K_1|$ dependencies are plotted in Fig. 6. Like in the case when the $[l,m,n]$ direction is along a hardest cubic anisotropy axis, there is a minimum in the $h_c(h)$ for positive K_1, but no minimum is observed in the corresponding dependence when $K_1<0$.

Representative δM plots for this case are shown in Fig. 7. It can be seen that δM plots obtained after thermal demagnetization are almost entirely positive, while δM^{ac} plots' shapes change significantly by increasing $K_u/|K_1|$ value for both positive and negative K_1. Initially, a minimum in each of these plots appears, becoming deeper with the K_u raise. For even greater $K_u/|K_1|$ the δM^{ac} plots turn to be entirely negative, with the minima becoming more shallow. Finally, for dominant uniaxial anisotropy, there are no deviations from the zero line.

D. $[l,m,n]$ given by [112] direction

The last case considered is the one when $[l,m,n]$ is along the [112] direction. This is used as an example for uniaxial anisotropy direction which does not coincide with the principal (easiest, hardest, or intermediate) cubic anisotropy axes. The h_c, h_r and M_r/M_s vs $K_u/|K_1|$ dependencies

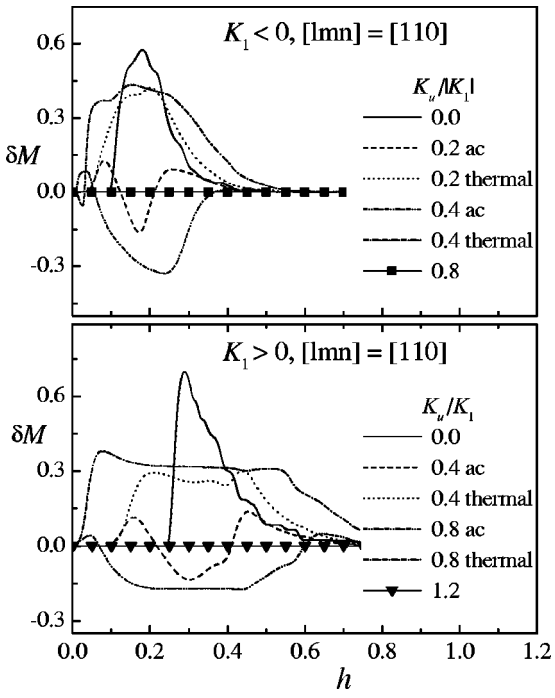

FIG. 7. Representative δM plots when the $[l,m,n]$ direction is along an intermediate cubic anisotropy axis.

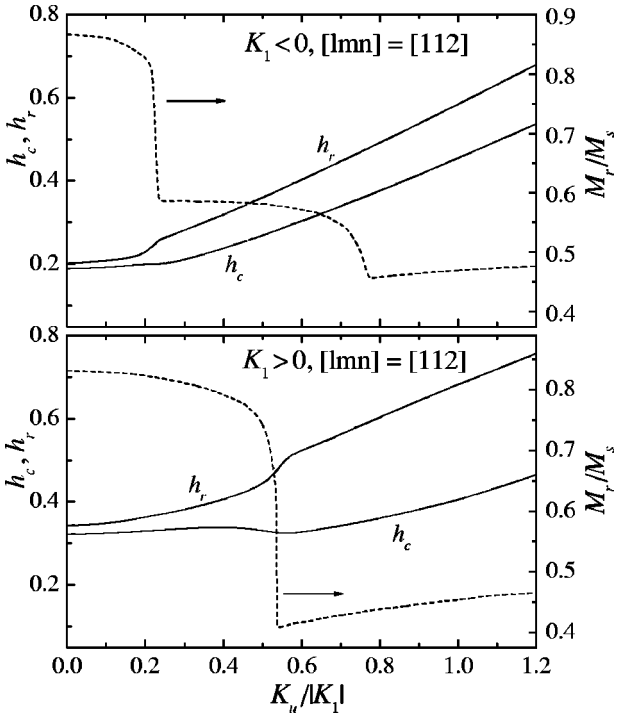

FIG. 8. Reduced coercivity, remanence coercivity, and saturation remanence vs $K_u/|K_1|$ for $[l,m,n]$ given by [112] direction.

are shown in Fig. 8. Like in the case discussed above, a shallow minimum in $h_c(h)$ for positive K_1 is observed, there is no minimum for negative K_1.

Some δM plots for this case are plotted in Fig. 9. The curves for positive K_1 are similar to those for $[l,m,n]$ along [110] direction. A variety of shapes is observed for $K_1<0$.

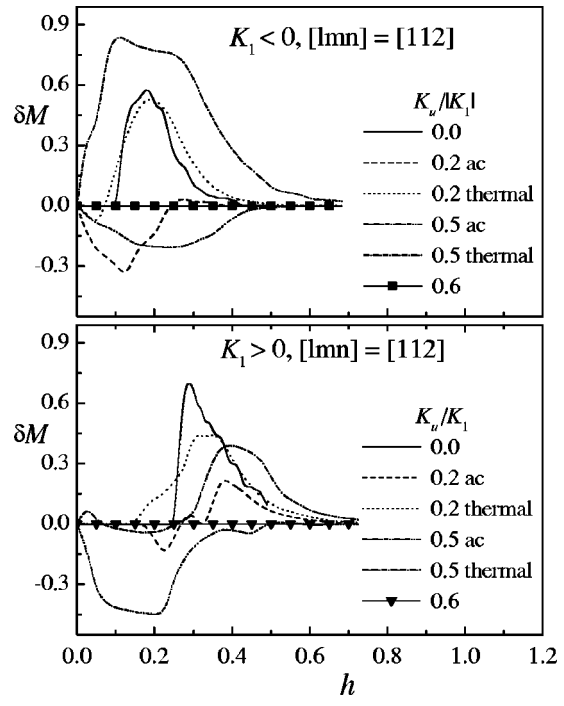

FIG. 9. Representative δM plots for $[l,m,n]$ along [112] direction.

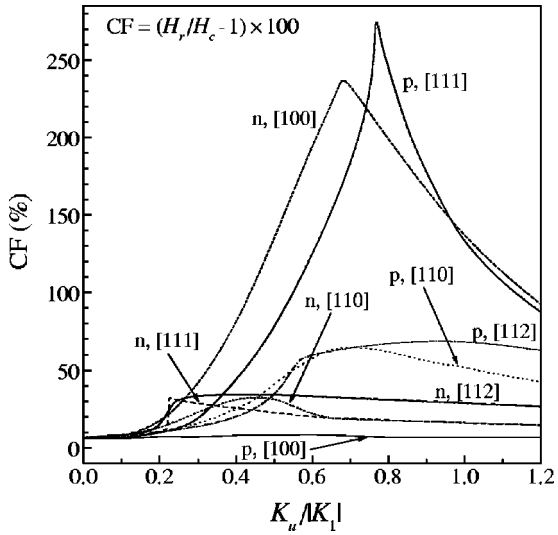

FIG. 10. Coercivity factor, CF, vs $K_u/|K_1|$ for several $[l,m,n]$ directions. The annotations *n* (negative) and *p* (positive) give the sign of K_1.

E. Coercivity factor

Figure 10 displays the dependencies of the coercivity factor, CF, on $K_u/|K_1|$ calculated for the above considered cases. All the plots show maxima, one of them reaching 275%, and note that there are no interparticle interactions. The highest values are for the cases when the minima in the reduced coercivity dependencies are the most pronounced.

Another important feature of this figure is the rather high CF even for $K_u/|K_1|$ sufficiently high so the uniaxial anisotropy is dominant, i.e., the number of minimum energy directions is reduced to 2, which is true for $K_u/|K_1|>1$ for any $[l,m,n]$ direction. This means that even for effectively ''uniaxial'' anisotropy particles, for which the δM plots are already zero line, the CF values can be rather higher than the value of 9% for Stoner–Wohlfarth particles.[16]

IV. CONCLUSIONS

The saturation remanence, coercivity, remanence coercivity, and coercivity factor values have been obtained for the cases when the uniaxial anisotropy direction is along the hardest, easiest and intermediate cubic anisotropy axes, as well as for one more case, $[l,m,n]$ given by [112] direction. The corresponding δM plots and CF vs $K_u/|K_1|$ dependencies have been constructed, considering non-interacting particles.

A variety of shapes of the remanence plots has been obtained when the uniaxial anisotropy does not dominate. CF values rather higher than the values for pure uniaxial or cubic anisotropy particles have been obtained as well, and even for dominating uniaxial anisotropy (when the anisotropy energy has only two minima), the CF can be very high for all cases considered here.

Thus, it has been shown that deviations from the zero line in the δM plots, or coercivity factor values different from the ones for the pure uniaxial or cubic anisotropy, cannot be directly attributed to interactions in the case of com-

peting anisotropies. A specific analysis must be applied for each particular case.

ACKNOWLEDGMENTS

This work has been supported by Conselho Nacional de Desenvolvimento Científico e Tecnológico (CNPq, Brazil), Fundação de Amparo à Pesquisa do Estado do Rio Grande do Sul (FAPERGS, Brazil), and Financiadora de Estudos e Projetos (FINEP, Brazil).

[1] E. P. Wohlfarth, J. Appl. Phys. **29**, 595 (1958).
[2] O. Henkel, Phys. Status Solidi **7**, 919 (1964).
[3] P. R. Bissel, R. W. Chantrell, G. Tomka, J. E. Knowles, and M. P. Sharrock, IEEE Trans. Magn. **25**, 3650 (1989).
[4] M. Fearon, R. W. Chantrell, and E. P. Wohlfarth, J. Magn. Magn. Mater. **86**, 197 (1990).
[5] M. Pardavi-Horvath, J. Oti, G. Vertesy, L. H. Bennett, and L. J. Swartzendruber, J. Magn. Magn. Mater. **104–107**, 313 (1992).
[6] P. E. Kelly, K. O'Grady, P. I. Mayo, and R. W. Chantrell, IEEE Trans. Magn. **2**, 3881 (1989).
[7] R. A. McCurie and P. Gaunt, Proceedings of the International Conference on Magnetism, Nottingham, 1964, p. 780.
[8] G. Bertotti and V. Basso, J. Appl. Phys. **73**, 5827 (1993).
[9] R. D. McMichael, F. Vajda, and E. Della Torre, J. Appl. Phys. **75**, 5692 (1994).
[10] K. J. Davies, S. Wells, R. V. Upadhyay, S. W. Charles, K. O'Grady, M. El Hilo, T. Meaz, and S. Mørup, J. Magn. Magn. Mater. **149**, 14 (1995).
[11] J. Geshev and M. Mikhov, J. Magn. Magn. Mater. **104–107**, 1569 (1992).
[12] A. D. C. Viegas, J. Geshev, L. F. Schelp, and J. E. Schmidt, J. Appl. Phys. **82**, 2466 (1997).
[13] D. G. Tonge and E. P. Wohlfarth, Philos. Mag. **3**, 536 (1958).
[14] A. S. Arrott, *Nanomagnetism*, edited by A. Hernando (Kluwer, Dordrecht, 1993), p. 73.
[15] J. Geshev, A. D. C. Viegas, and J. E. Schmidt, J. Appl. Phys. **84**, 1488 (1998).
[16] A. R. Corradi and E. P. Wohlfarth, IEEE Trans. Magn. **14**, 861 (1978).